VOL. 22, NO. 1, 2023, 83-87
www.fke.utm.my/elektrika
ISSN 0128-4428

ELEKTRIKA
Journal of Electrical Engineering

Simulation of Prostate Specific Antigen ISFET Sensor With Different Nanostructures

Lee Shung Mun, Suhana Mohamed Sultan* and **Nur Afiqah Ab Razak**

Faculty of Electrical Engineering, Universiti Teknologi Malaysia, 81310 UTM Skudai, Johor, Malaysia.

*Corresponding author: suhana@fke.utm.my

Abstract: It is crucial to have early detection of prostate cancer as it is the third most common cancer in men and Prostate Specific Antigen (PSA) is a protein-based biomarker commonly used to achieve the purpose. Besides, ISFET integrated with nanostructures such as nanowire and nanosphere has been the focus of research for disease diagnosis. Simulations are carried out in Biosensor Lab to investigate the performance of ISFET with planar, nanowire and nanosphere structures in detecting PSA. Using nanostructured ISFET in disease diagnosis is demonstrated by comparing the performance with the surface-to-volume (S/V) ratio. The nanosphere biosensor with the highest S/V ratio showed the lowest settling time when there was a low analyte concentration. Its settling time is 788 times lower than planar and almost 3 times lower than nanowire ISFET. In addition, the time needed for a planar biosensor to capture $\mathbf{1\times10^{9}}$ M of PSA is 5 times slower than a nanowire biosensor and nanosphere biosensor. In signal-to-noise ratio (SNR), nanosphere ISFET exhibits the highest value compared to other structures. These results indicate that a higher S/V ratio contributed to better performance in detecting PSA.

Keywords: Biosensor Lab, Ion-sensitive field-effect transistor, Prostate Specific Antigen, receptor density, settling time

Article History: received 23 August 2022; accepted 29 November 2022; published 28 April 2023.

1. INTRODUCTION

Ultrafast diagnosis platforms will be the trend in the future in the medical field and highly sensitive electoral detection of biomarkers plays an important role in the early-stage screening of many deadly diseases. The Covid-19 pandemic especially, showed us how important it is to detect a disease in the early stage. A fast and accurate diagnosis would help the patient to get proper timely treatment and slow down the speed of spreading [1]. There are many laboratory-based techniques that are being used in the detection and diagnosis of infectious diseases and are well-established. These techniques include Polymerase Chain Reaction (PCR), microscopies, and immunoassays [2]. However, they have shown shortages when dealing with the high demand for fast and accurate screening of the mass population during pandemic. Thus, this led to the blooming of biosensing innovations towards miniaturized devices that are affordable to all and provides accurate and early detection of diseases.

Glucose at-home test by using a potentiometric sensor is the best example showing the advantages of having a small-sized device [3]. Different configurations are available for the test, and this helps to monitor the health status of diabetic patients so that early consultation can be carried out when needed. Furthermore, biosensors also can be used for screening various diseases by detecting the reaction of antigen, DNA, enzymes, or protein with the sensing surface. This makes biosensors the desired solution in helping the patient to obtain appropriate therapy in the early stage.

Cancer is one of the main causes of death globally with 18.1 million new cases and 9.6 million deaths reported in 2018 [4]. In 2020, it is observed that prostate cancer contributed to 7.3% of all cancer cases [5]. While in Malaysia, prostate cancer is the third most common cancer in men and 1 out of 117 will have a risk of having prostate cancer. Thus, it is important to have early detection so that treatment can be carried out in the early stage and improve the survival rate of patients [6]. PSA is a protein-based biomarker that is commonly used for screening prostate cancer. It is secreted by the epithelial cells of the prostate and the abnormal concentration level of it can be used as an early sign of prostate cancer [7]. Thus, it is important to have an effective biosensor that is able to detect protein-based PSA.

Ion-sensitive field-effect transistor (ISFET) is a popular biosensor technology in recent decades. Among all the different structures, ISFET integrated with nanostructures such as nanowire and nanosphere has attracted more interest to be used in disease diagnosis of disease [8, 9]. This is mainly because nanostructured ISFET have a higher surface-to-volume ratio and are more sensitive to the changes in electrochemical properties during label-free sensing [10]. Thus, the aim of this work is to compare the performance of different dimensional nanostructure-based ISFET biosensor in terms of the settling time and selectivity. The design and analysis were conducted using the Biosensor lab from nanohub.org [11].

2. BIOSENSOR SIMULATION

2.1 Design Parameters

Table 1 presents the nanostructure design parameters that have been set for the simulation of the biosensor. The dimensions of the nanowire are selected based on the device's best performance shown in [12].

Table 1. Nanostructure Design Parameters used in Biosensor Simulation

Type of nanostructure	No	Parameters	Values
Planar	1.	Length (nm)	100//5
	2.	Width (nm)	100//5
Nanowire	1.	Diameter (nm)	70 //1
	2.	Length (nm)	100
Nanosphere	1.	Diameter (nm)	100//1

Based on the values, the parameters for planar and nanosphere biosensor is set such that the device will have similar width when compared to nanowire biosensor. Other physical parameters such as oxide thickness and doping concentration were set at 1 nm and $1\times10^{19}cm^{-3}$, respectively. Figure 1 shows the device design for all three nanostructures.

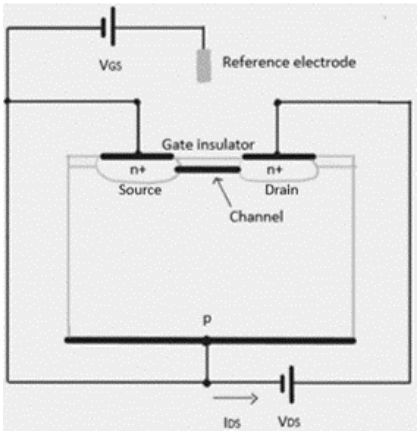

(a)

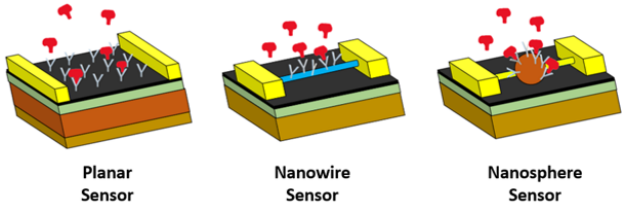

(b)

Figure 1. (a) General structure of an ISFET (b) Design for all three structures; planar, nanowire and nanosphere.

2.1 Simulation Parameters

Table 2 presents the simulation settings for both settling time and selectivity analysis which are set prior to the biosensing simulation. The simulation parameters are taken from Ref [13]. The target analyte molecule is set to be the PSA for the simulation. The anti-PSA antibody is set as the receptor in the simulation setting. It is required to analyze the settling time against the analyte concentration with a certain range of analyte concentration and at a specific target analyte concentration for transient response analysis.

In the analysis for selectivity, a graph of SNR against the receptor density is obtained. Apart from these parameters, the size of parasitic molecules is set to 1 nm to study the selectivity of each biosensor device. However, the target molecule concentration is set to be significantly lower than the parasitic molecules. This will aid the study of each biosensor with different nanostructures to detect the presence of the target biomolecule. Note that for all the simulations, the diffusion coefficient, which is the rate of diffusion of the PSA molecules is set to be at $8.5\times10^{-7}cm^2/s$.

Table 2. Nanostructure Biosensor Simulation Settings

Measurement	No	Simulation Settings	Values
Settling time vs Analyte Concentration	1.	Lower value of analyte concentration (molar units)	1×10^{-15}
	2.	Upper value of analyte concentration (molar units)	1×10^{-6}
Time-dependent Capture of Target Molecules	1.	Target analyte concentration (molar units)	1×10^{-9}
	2.	Start time for transient response (s)	1×10^{-6}
	3.	Final time for transient response (s)	1×10^{5}
	4	Steps	100
Signal-to-Noise Ratio (SNR) vs Receptor Density	1.	Size of parasitic molecules (nm)	1
	2.	Concentration of target molecules (molar units)	1×10^{-12}
	3.	Concentration of parasitic molecules (molar units)	1×10^{-6}
	4.	Lower value of receptor density (unit/cm^2)	1×10^{11}
	5.	Upper value of receptor density (unit/cm^2)	5×10^{12}

2.2 Simulation Model

Biosensor lab is a numerical simulator that focuses on electrostatic nanobiosensing and follows "lock and key" principle. In simulations for settling time for biosensors, the Diffusion-Capture Model is used to describe the

process of molecule capture. The model assumes that molecule transport is diffusion-limited and target-receptor conjugation is treated as first order reaction [14]. The equations are shown below,

$$\frac{d\rho}{dt} = D\nabla^2\rho \quad (1)$$

$$\frac{dN}{dt} = k_F(N_0 - N)\rho_s - k_R N(1b) \quad (2)$$

where ρ is concentration of target molecules in solution, and D is the diffusion coefficient of target molecules in Equation 1 while N is the density of conjugated receptors, N_0 is the total density of receptors on sensor surface, k_F and k_R are the capture and dissociation constants, and ρ_s is the concentration of target analyte on sensor surface in Equation 2.

Simulation for SNR modelled as the ratio of available binding sites for target molecule (N_0) to the density of possible locations for parasitic absorption (N_ρ) [15]. The equation is obtained based on the consideration of random sequential absorption (RSA) combined with kinetics of diffusion limited Langmuir process,

$$\frac{dN}{dt} = k_F(N_0 - N)\rho_s - k_R N(1b) \quad (2)$$

where σ_T/σ_ρ denotes the ratio of electrostatic charge of target molecule to parasitic molecule, k_T/k_ρ denotes the ratio of reaction constant (k_F/k_R) of target molecule to parasitic molecule, and ρ_T/ρ_ρ represents the ratio of density of target molecule to parasitic molecule at the surface. In the simulation, target molecules and parasitic molecules is assumed to have same incubation time and diffusion is one dimensional towards the surface. Thus, effect of concentrations on SNR can be accurately analyzed.

3. DISCUSSION

Figure 2 shows the results of settling time against the analyte concentration for different structures. From the graph, it can be observed that all devices' settling time decreases as analyte concentration increases. For example, from the plot, the nanosphere biosensor with a higher S/V ratio showed the lowest settling time when there was a low analyte concentration.

This behavior can be related to each nanostructure's S/V ratio. Table 3 presents the value of the S/V ratio of each nanostructure with its respective settling time in the biosensing simulation. Figure 3 shows the respective plot of settling time with the S/V ratio of the nanostructures. As the S/V ratio increases, the trend of settling time decreases. Thus, to produce a device with a faster response, the S/V ratio of the device needs to be increased.

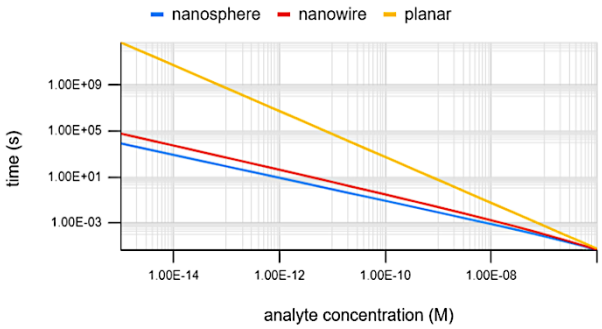

Figure 2. Plot of settling time against the analyte concentration.

Table 3. Nanostructure Biosensor Simulation Settings

Device	Surface-to-Volume Ratio	Settling time at $1\times10^{-9}M$ of analyte concentration (s)
Planar*	$\frac{(100\times10^{-9})^2}{(100\times10^{-9})^2\times t} = \frac{1}{t}$	7.094
Nanowire	$\frac{2}{35\times10^{-9}} = 5.71\times10^{7}$	0.026
Nanosphere	$\frac{3}{50\times10^{-9}} = 6\times10^{7}$	0.009

*t is defined as the thickness for the planar device. The value t is assumed to be $t \gg$ radius of the nanowire and nanosphere, thus the S/V ratio is smaller.

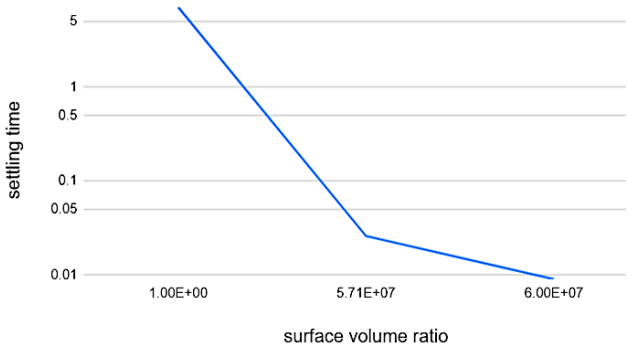

Figure 3. Plot of settling time against S/V ratio, at analyte concentration of $1\times10^{-9}M$. The unit for settling time is in second (s).

This is because as the S/V ratio increases, the surface exposed to the analyte will be larger and more target molecules can be captured in the same period. Thus, nanosphere ISFET showed the lowest settling time compared to planar and nanowire ISFET. Its settling time is 788 times lower than planar and almost 3 times lower than nanowire ISFET.

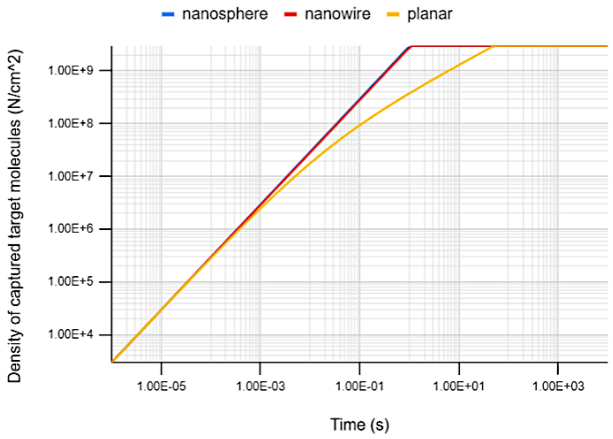

Figure 4. Plot of the density of captured target molecule against time

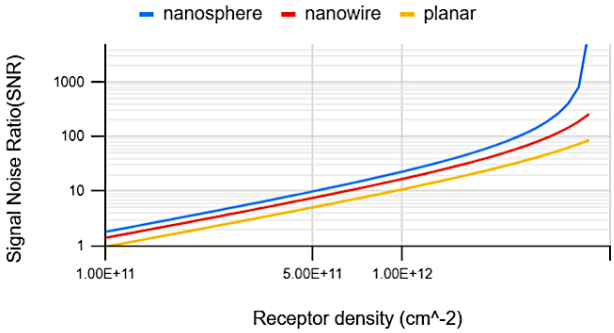

Figure 5. Plot of SNR against receptor density

Figure 4 shows the combined graph of the density of captured target molecules against time for all devices used in this work. This graph shows the biosensor's speed in capturing a specific concentration of target molecules. In this project, the target molecule was PSA. Figure 4 shows that the time needed for a planar biosensor to capture 1×10^9 M of the PSA is more than 1 second, while nanowire biosensor and nanosphere biosensor only takes around 0.2 seconds to achieve the same result. This shows that the planar biosensor is more than 5 times slower than this project's other devices. Nanowire and nanosphere shows similar pattern because the difference in surface area between nanosphere and nanowire is small compared to the planar biosensor.

Figure 5 shows the plot of the SNR against the receptor density for each nanostructure device. This graph shows the selectivity attributes of the ISFET sensor. It is observed that as receptor density increases, the SNR of all the devices will increase. This is because when more receptor is available, target molecules will be easier to capture even with a high concentration of parasitic molecules. This translates to a device with higher resistance to parasitic molecules with increased receptor density. Selectivity is highly related to the S/V ratio of a device.

From Figure 5, it can be observed that the nanosphere ISFET exhibits the highest SNR compared to other structures. This is because the higher S/V ratio of nanosphere ISFET enables receptors of the same density to have higher exposure to the analyte, thus increasing the resistance to parasitic molecules. This can be seen in other structure that has high S/V ratio as well [10].

4. CONCLUSION

Nanosphere biosensor showed the best performance in settling time and selectivity when compared to planar and nanowire biosensor. The settling time of the nanosphere biosensor is 788 times lower compared to planar and is 3 times lower compared to the nanowire. Planar biosensor takes 5 times longer time to capture 1×10^9 M of PSA compared to nanowire and nanosphere biosensor. Besides, nanosphere biosensor showed better resistance to parasitic molecules by showing a higher SNR when compared to other biosensors. The comparisons showed that a higher S/V ratio contributed to better performance in the detection of PSA.

ACKNOWLEDGMENT

This work was supported by the Ministry of Higher Education under Fundamental Research Grant Scheme (FRGS/1/2018/TK04/UTM/02/41) with UTM cost centre no. R.J130000.7851.5F053.

REFERENCES

[1] E. Mahase, "Covid-19: What have we learnt about the new variant in the UK?," BMJ, vol. 371, p. m4944, 2020, doi: 10.1136/bmj.m4944.

[2] A. O. Oyewole et al., "COVID-19 Impact on Diagnostic Innovations: Emerging Trends and Implications," Diagnostics, vol. 11, no. 2, p. 182, 2021. [Online]. Available: https://www.mdpi.com/2075-4418/11/2/182.

[3] M. Adeel, M. M. Rahman, I. Caligiuri, V. Canzonieri, F. Rizzolio, and S. Daniele, "Recent advances of electrochemical and optical enzyme-free glucose sensors operating at physiological conditions," Biosensors and Bioelectronics, vol. 165, p. 112331, 2020/10/01/ 2020, doi: https://doi.org/10.1016/j.bios.2020.112331.

[4] F. Bray, J. Ferlay, I. Soerjomataram, R. L. Siegel, L. A. Torre, and A. Jemal, "Global cancer statistics 2018: GLOBOCAN estimates of incidence and mortality worldwide for 36 cancers in 185 countries," (in eng), CA Cancer J Clin, vol. 68, no. 6, pp. 394-424, Nov 2018, doi: 10.3322/caac.21492.

[5] E. M. Ferlay J, Lam F, Colombet M, Mery L, Piñeros M, Znaor A, Soerjomataram I, Bray, "Global Cancer Observatory: Cancer Today." https://gco.iarc.fr/today (accessed 18 May, 2022).

[6] J. Lim et al., "Prostate cancer in multi-ethnic Asian men: Real-world experience in the Malaysia Prostate Cancer (M-CaP) Study," (in eng), Cancer Med, vol. 10, no. 22, pp. 8020-8028, Nov 2021, doi: 10.1002/cam4.4319.

[7] V. M. Velonas, H. H. Woo, C. G. dos Remedios, and S. J. Assinder, "Current status of biomarkers for prostate cancer," (in eng), Int J Mol Sci, vol. 14, no. 6, pp. 11034-11060, 2013, doi: 10.3390/ijms140611034.

[8] A. Poghossian and M. J. Schöning, "Recent progress in silicon-based biologically sensitive field-effect devices," Current Opinion in Electrochemistry, vol. 29, p. 100811, 2021/10/01/ 2021, doi: https://doi.org/10.1016/j.coelec.2021.100811.

[9] M. R. Hasan et al., "Recent development in electrochemical biosensors for cancer biomarkers detection," Biosensors and Bioelectronics: X, vol. 8,

p. 100075, 2021/09/01/ 2021, doi: https://doi.org/10.1016/j.biosx.2021.100075.

[10] A. Tarasov, W. Fu, O. Knopfmacher, J. Brunner, M. Calame, and C. Schoenenberger, "Signal-to-noise ratio in dual-gated silicon nanoribbon field-effect sensors," Applied Physics Letters - APPL PHYS LETT, vol. 98, 10/15 2010, doi: 10.1063/1.3536674.

[11] J. G. P. Nair, and M. Alam. "BioSensorLab User Manual." https://nanohub.org/resources/20854/download/User_Manual_1.pdf (accessed 11 April, 2022).

[12] M. Jadhav, S. Bhamare, V. Chauhan, S. Rao, N. Desai, and S. Subramaniam, "Design Optimization and Implementation of Nanowire Based Biosensors," in 2021 2nd Global Conference for Advancement in Technology (GCAT), 1-3 Oct. 2021 2021, pp. 1-6, doi: 10.1109/GCAT52182.2021.9587494.

[13] B. Shobha and N. Muniraj, "Design, Modeling and Simulation of Prostate Cancer Biosensor with ssDNA biomarker and DGFET Biosensor," IJCSIT, vol. 5, pp. 2612-2262, 2014

[14] P. R. Nair and M. A. Alam, "Screening-Limited Response of NanoBiosensors," Nano Letters, vol. 8, no. 5, pp. 1281-1285, 2008/05/01 2008, doi: 10.1021/nl072593i.

[15] P. R. Nair and M. A. Alam, "Theory of "Selectivity" of label-free nanobiosensors: A geometro-physical perspective," (in eng), J Appl Phys, vol. 107, no. 6, pp. 64701-64701, 2010, doi: 10.1063/1.3310531.